Dynamical Description of Coulomb Dissociation*

S. Typel and H. H. Wolter

Sektion Physik, Universität München, Am Coulombwall 1, D-85748 Garching

Z. Naturforsch. **54 a,** 63–76 (1999); received November 21, 1998

We present a simple and efficient method for a fully dynamical treatment of Coulomb excitation in the semiclassical approximation by solving the time-dependent Schrödinger equation. It allows to investigate the importance of higher order effects in the breakup process. The method is applied to the Coulomb breakup of ^{7}Li scattered on ^{197}Au at 42 MeV projectile energy.

Key words: Coulomb Dissociation; Higher Order Effects.

1. Introduction

The Coulomb dissociation of light nuclei in the scattering on highly charged targets has attracted much attention in recent years. It can give valuable information on the structure of exotic nuclei and permits the extraction of astrophysical S-factors for the inverse radiative capture reaction, see, e. g., the review articles [1] for a detailed discussion. In order to get reliable information, the mechanism of the breakup process has to be fully understood and the validity of the theoretical description has to be established. The difficulty is that the very low energy radiative capture reactions can safely be discribed by a first-order E1- or E2-process, while the high-energy dissociation reaction includes higher orders, which can be seen a post-acceleration of the fragments in the Coulomb field of the target.

A fully dynamical calculation includes all higher order effects, and we can obtain a clear concept of the time evolution of the excitation process. A visualization of the time-dependent spatial distribution of the projectile wave function is especially helpful. In the problem of Coulomb dissociation, the time-dependent method is a viable method to other approaches, like explicit higher-order [2] or coupled-channels calculations [3]. However, the visualization of scattering or reaction wave functions is an interesting problem in its own right. The visualization of the quantum-mechanical evolution may lead to new and more efficient approximations. This is particularly relevant now with the study of very weakly-bound systems, where the continuum is always very close. Conventional direct reaction methods can usually not be applied here.

The interpretation and visualization of the ψ-function has been of particular interest to G. Süßmann [4]. Some time ago he has initiated a study by one of the authors on the fusion process also described as a time-dependent problem [5]. Thus it is appropriate to dedicate this article to G. Süßmann on his 70$^{\text{th}}$ birthday.

Returning to Coulomb dissociation, in the case of heavy targets and for small scattering angles of the projectile, the breakup process is dominated by the strong Coulomb force as compared to the nuclear induced breakup which we will neglect in our calculation. Our theoretical description is then based on the semiclassical approximation [6], i. e. the motion of the projectile in the Coulomb field of the target is treated classically and the excitation of the projectile is calculated quantummechanically. The semiclassical approximation is valid as long as the Sommerfeld parameter

$$\eta = \frac{Z_a Z_X e^2}{\hbar v} \tag{1}$$

is large compared to one. Here Z_a and Z_X are the charge numbers of projectile a and target X, and v is the initial velocity of the projectile. Another important quantity is the adiabaticity parameter

$$\xi = \frac{\omega b}{v}, \tag{2}$$

* Dedicated to Georg Süßmann on occasion of his 70th birthday.

Reprint requests to Prof. H. Wolter; Fax: +49 89 2891 4008; E-mail: hermann.wolter@physik.uni-muenchen.de.

0932–0784 / 99 / 0100–0063 $ 06.00 © Verlag der Zeitschrift für Naturforschung, Tübingen · www.znaturforsch.com

Dieses Werk wurde im Jahr 2013 vom Verlag Zeitschrift für Naturforschung in Zusammenarbeit mit der Max-Planck-Gesellschaft zur Förderung der Wissenschaften e.V. digitalisiert und unter folgender Lizenz veröffentlicht: Creative Commons Namensnennung-Keine Bearbeitung 3.0 Deutschland Lizenz.

This work has been digitalized and published in 2013 by Verlag Zeitschrift für Naturforschung in cooperation with the Max Planck Society for the Advancement of Science under a Creative Commons Attribution-NoDerivs 3.0 Germany License.

Zum 01.01.2015 ist eine Anpassung der Lizenzbedingungen (Entfall der Creative Commons Lizenzbedingung „Keine Bearbeitung") beabsichtigt, um eine Nachnutzung auch im Rahmen zukünftiger wissenschaftlicher Nutzungsformen zu ermöglichen.

On 01.01.2015 it is planned to change the License Conditions (the removal of the Creative Commons License condition "no derivative works"). This is to allow reuse in the area of future scientific usage.

where $\hbar\omega$ is the excitation energy of the projectile system and b is the impact parameter. The adiabaticity parameter compares the time of interaction $\frac{b}{v}$ with the typical nuclear period ω^{-1}. A sufficiently large excitation probability can only be expected for ξ smaller then one. From (2) we see that small excitation energies and impact parameters favour a strong excitation.

Coulomb excitation probabilities are generally calculated in simple approximations where the dynamical evolution of the projectile scattering wave is not fully considered. The standard approach is the expansion of the excitation amplitude into a perturbation series in powers of the target charge $Z_X e$ [6]. Usually only the first order contribution is considered, corresponding to a one-photon exchange between projectile and target. This method definitely neglects higher order contributions from multiple-photon exchange. The inclusion of higher order contributions in the perturbation series is possible in an approximation for small ξ [2] but it is rather limited with respect to actual experimental conditions.

While finite excitation energies are taken into account in the perturbation approach, the sudden approximation, on the other hand, assumes an instantaneous excitation process, i. e. $\xi = 0$, corresponding to an energetic degeneracy of all states involved. Here, higher order effects are taken into account to all orders, but the method is only applicable for very fast collisions.

In order to study the excitation process under general conditions of projectile energy, scattering angle and excitation energy a full dynamical treatment of the time evolution of the projectile system during the collisions is necessary. Therefore the time-dependent Schrödinger equation with an explicit time-dependent perturbation has to be solved in the semiclassical approximation. This is a rather involved computational task, and convenient numerical techniques are required.

The Coulomb dissociation process of projectiles like ^{8}B, ^{11}Li and ^{11}Be has been treated in the framework of the time-dependent Schrödinger equation before [7 - 11] but mostly under some simplified assumptions at large projectile energies. E. g. one- and two-dimensional models in coordinate space were investigated, a straight-line trajectory of the projectile was assumed, which is only valid for high energy collisions, only E1 excitation was considered or the spin of the particles was neglected in the nuclear models used. Even with these simplifications the calculations gave an indication of the effects of higher order contributions. We will describe a method which is less restrictive than most of the earlier calculations in order to get results which are comparable to experimental data.

The paper is organized as follows. In Sect. 2 we describe a general method for solving the time-dependent Schrödinger equation which can be used whenever the problem depends on one (three-dimensional) dynamical variable, the potentials involved are local and the initial state can be represented by a normalized wave function localized in space. In Sect. 3 the method is specialized to the case of the semiclassical approximation to Coulomb dissociation assuming a simple two-body model of the projectile system. The method is applied in Sect. 4 to the Coulomb breakup of 42 MeV ^{7}Li scattered on ^{197}Au, which corresponds to the conditions of a recent experiment [12]. We close in Sect. 5 with a summary and conclusions.

2. Solving the Time-Dependent Schrödinger Equation

We assume that the system under investigation can be described by the wave function

$$\Psi(\vec{r},t) = \sum_c \frac{\psi_c(r,t)}{r} \langle \hat{r}|c\rangle \tag{3}$$

where $\vec{r}$ is the dynamical variable. The dependence of the wave function on $r = |\vec{r}|$ is given by the time-dependent radial functions $\psi_c(r,t)$. The index c stands for an individual channel, which is characterized by the quantum numbers (J_c, M_c, l_c, s_c). The spin and angular dependence of the wave function is contained in the functions

$$\begin{aligned}\langle \hat{r}|c\rangle &= \mathcal{Y}^{l_c s_c}_{J_c M_c}(\hat{r}) \\ &= \sum_{m_l m_s} (l_c m_l s_c m_s | J_c M_c) Y_{l_c m_l}(\hat{r}) \chi_{s_c m_s},\end{aligned} \tag{4}$$

where the orbital angular momentum l_c is coupled with the channel spin s_c to the total angular momentum J_c.

2.1. *The Unperturbed System*

The dynamics of the unperturbed stationary system is given by the Hamiltonian

$$\boldsymbol{H}_0 = \frac{p^2}{2\mu} + \sum_{c'c} |c'\rangle V_0^{c'c}(r)\langle c|, \tag{5}$$

where we allow for a coupling between different channels by local potentials $V_0^{c'c}(r)$, e. g. through spin-orbit or tensor forces. Solutions of the time-dependent Schrödinger equation

$$i\hbar\frac{\partial}{\partial t}\boldsymbol{\Phi}(\vec{r},t) = \boldsymbol{H}_0(\vec{r})\boldsymbol{\Phi}(\vec{r},t) \tag{6}$$

are given by

$$\boldsymbol{\Phi}(\vec{r},t) = \phi(\vec{r})\exp\left(\frac{Et}{i\hbar}\right), \tag{7}$$

where

$$\phi(\vec{r}) = \sum_c \frac{\phi_c(r)}{r}\langle\hat{r}|c\rangle \tag{8}$$

is a solution of the stationary Schrödinger equation

$$\boldsymbol{H}_0(\vec{r})\phi(\vec{r}) = E\phi(\vec{r})\,. \tag{9}$$

The functions $\phi(\vec{r})$ are assumed to be known by solving the eigenvalue equation, i. e. by a diagonalisation of the Hamiltonian $\boldsymbol{H}_0$.

2.2. *The System with Time-Dependent Perturbation*

The action of an external time-dependent perturbation can be described by adding a potential

$$V(\vec{r},t) = \sum_{c'c}\langle\hat{r}|c'\rangle V^{c'c}(r,t)\langle c| \tag{10}$$

to the free Hamiltonian $\boldsymbol{H}_0$. This leads to the total Hamiltonian

$$\boldsymbol{H}(\vec{r},t) = \boldsymbol{H}_0(\vec{r}) + V(\vec{r},t)\,. \tag{11}$$

In general it is very difficult to find a solution of the time-dependent Schrödinger equation

$$i\hbar\frac{\partial}{\partial t}\boldsymbol{\Psi}(\vec{r},t) = \boldsymbol{H}(\vec{r},t)\boldsymbol{\Psi}(\vec{r},t) \tag{12}$$

if the Hamiltonian is explicitly time-dependent. Inserting (3,5,10,11) into (12) and projecting on channel $\langle c'|$ we obtain for the time-dependent Schrödinger equation the set of equations

$$i\hbar\frac{\partial}{\partial t}\psi_{c'}(r,t) = \sum_c h_{c'c}(r,t)\psi_c(r,t)\,, \tag{13}$$

where we have introduced the abbreviation

$$h_{c'c}(r,t) = \Big[-\frac{\hbar^2}{2\mu}\Big(\frac{\partial^2}{\partial r^2} - \frac{l_c(l_c+1)}{r^2}\Big)\delta_{c'c} + \Big(V_0^{c'c}(r) + V^{c'c}(r,t)\Big)\Big]\,. \tag{14}$$

Then the solution of the reduced time-dependent Schrödinger equation (13) can be written:

$$\psi_{c'}(r,t) = \psi_{c'}(r,t_i) + \frac{1}{i\hbar}\int_{t_i}^{t} \mathrm{d}\,t' \sum_c h_{c'c}(r,t')\psi_c(r,t'). \tag{15}$$

For a small time step Δt we have the approximation

$$\psi_{c'}(r,t+\Delta t) \approx \psi_{c'}(r,t) + \frac{\Delta t}{i\hbar}\sum_c h_{c'c}(r,t)\psi_c(r,t)\,. \tag{16}$$

2.3. *Numerical Solution of the Time-Dependent Schrödinger Equation*

The simple form (16) is the starting point for the numerical solution of the initial value problem. The radial wave function in each channel c is discretized

$$\psi_c(r,t) \to \vec{\psi}_c(t) = \big[\psi_c(r_0,t), \psi(r_1,t), \ldots, \psi(r_{n-1},t)\big] \tag{17}$$

on a mesh with n points and constant step size $h = r_{i+1} - r_i$. For the total wave function we introduce the vector

$$\boldsymbol{\psi}(t) = \big[\vec{\psi}_1(t), \ldots, \vec{\psi}_{n_c}(t)\big]\,,\ \text{i. e. } [\boldsymbol{\psi}(t)]_{c,i} = \psi_c(r_i,t) \tag{18}$$

This vector has $N = n \times n_c$ entries when n_c is the number of channels. Using the finite difference approximation

$$\frac{\partial^2}{\partial r^2}\psi_c(r_i,t) \approx \frac{\psi_c(r_{i+1},t) - 2\psi_c(r_i,t) + \psi_c(r_{i-1},t)}{h^2}, \tag{19}$$

we can write the time dependent Schrödinger equation for the wave function $\psi(t)$ in "matrix" form

$$i\hbar\frac{\partial}{\partial t}\psi(t) = \mathbf{h}(t)\psi(t), \tag{20}$$

where the matrix $\mathbf{h}(t)$ has indices c', c, i and j

$$[\mathbf{h}(t)]_{c'cij} = \begin{cases} [-\frac{\hbar^2}{2\mu}(-\frac{2}{h^2} - \frac{l_c(l_c+1)}{r_i^2})]\delta_{c'c} \\ + \left(V_0^{c'c}(r_i) + V^{c'c}(r_i,t)\right) & \text{if } i = j, \\ -\frac{\hbar^2}{2\mu}\frac{1}{h^2}\delta_{c'c} & \text{if } |i-j| = 1, \\ 0 & \text{if } |i-j| > 1. \end{cases} \tag{21}$$

For small time steps we can approximate (20) as

$$\psi(t+\Delta t) \approx \frac{\mathbf{1} + \frac{\Delta t}{2i\hbar}\mathbf{h}(t)}{\mathbf{1} - \frac{\Delta t}{2i\hbar}\mathbf{h}(t)}\psi(t), \tag{22}$$

which is identical to equation (16) to first order in Δt. The matrix

$$\mathbf{U}(t) = \frac{\mathbf{1} + \frac{\Delta t}{2i\hbar}\mathbf{h}(t)}{\mathbf{1} - \frac{\Delta t}{2i\hbar}\mathbf{h}(t)}, \tag{23}$$

introduced in (22), has the advantage of being unitary so that the modulus of the wave function stays constant during the time integration [13]. If we define the auxiliary vector

$$\chi(t) = \frac{1}{2}[\psi(t) + \psi(t+\Delta t)], \tag{24}$$

we find a system of linear equations, first,

$$\mathbf{A}(t)\chi(t) = \psi(t) \quad \text{with} \quad \mathbf{A}(t) = \left[\mathbf{1} - \frac{\Delta t}{2i\hbar}\mathbf{h}(t)\right] \tag{25}$$

for the unknown $\chi(t)$, and finally

$$\psi(t+\Delta t) = 2\chi(t) - \psi(t)\,. \tag{26}$$

For each time step the system of inhomogeneous linear equations (25) has to be solved, which is in general rather time-consuming because of the large dimension of the matrix $\mathbf{A}$. Considering the structure of the matrix $\mathbf{h}(t)$ in (21), the system (25) can be written in a form with a tridiagonal matrix of dimension $n \times n$ with entries which are matrices of dimension $n_c \times n_c$. This allows for a fast solution of the inhomogeneous system of linear equations (25) with a Gaussian elimination method [5, 13].

For this purpose we define the $n \times n$ matrix $\mathbf{B}$ by

$$[\mathbf{B}(t)]_{ij} := \mathbf{C}_{ij}(t), \tag{27}$$

where $\mathbf{C}_{ij}$ are $n_c \times n_c$ matrices with

$$[\mathbf{C}_{ij}(t)]_{c'c} = \delta_{c'c}\delta_{ij} - \frac{\Delta t}{2i\hbar}\mathbf{h}_{c'cij}(t)\,. \tag{28}$$

Accordingly, we exchange the ordering of the elements in the vectors ψ and χ. We introduce the vectors $\mathbf{X}(t)$ and $\mathbf{Y}(t) = \frac{1}{2}(\mathbf{X}(t) + \mathbf{X}(t+\Delta t))$ by

$$[\mathbf{X}(t)]_i = \vec{\chi}(t)_i \quad \text{with} \quad [\vec{\chi}(t)_i]_c = \psi_c(r_i, t). \tag{29}$$

Instead of (25,26) we now find the system of linear equations

$$\mathbf{B}(t)\mathbf{Y}(t) = \mathbf{X}(t) \tag{30}$$

for the unknown $\mathbf{Y}(t)$ and finally

$$\mathbf{X}(t+\Delta t) = 2\mathbf{Y}(t) - \mathbf{X}(t)\,. \tag{31}$$

The matrix $\mathbf{B}$ has a tridiagonal structure with $[\mathbf{B}(t)]_{ij} = \mathbf{C}_{ij}(t) = \mathbf{0}$ for $|i-j| > 1$. The system (30) can now be solved by the following procedure with n matrices $\mathbf{F}_i(t)$ and $\mathbf{G}_i(t)$ of dimension $n_c \times n_c$ and n vectors $\mathbf{f}_i(t)$ and $\mathbf{g}_i(t)$ with n_c elements (the argument t is suppressed in the following):

1. Define

$$\mathbf{G}_0 = \mathbf{B}_{00}^{-1}\mathbf{B}_{01} \quad \text{and} \quad \mathbf{g}_0 = \mathbf{B}_{00}^{-1}X_0.$$

2. Calculate recursively for $i = 1, \ldots, n-1$:

$$\begin{aligned} \mathbf{F}_i &= \mathbf{B}_{ii} - \mathbf{B}_{ii-1}\mathbf{G}_{i-1}, \\ \mathbf{f}_i &= \mathbf{X}_i - \mathbf{B}_{ii-1}\mathbf{g}_{i-1}, \\ \mathbf{G}_i &= \mathbf{F}_i^{-1}\mathbf{B}_{ii+1}, \quad \text{only for } i \le n-2, \\ \mathbf{g}_i &= \mathbf{F}_i^{-1}\mathbf{f}_i. \end{aligned}$$

With these operations the matrix $\mathbf{B}$ is transformed to an upper triangular matrix $\mathbf{G}$ with unit diagonal entries (upper Hessenberg matrix).

3. The transformed equations $\mathbf{GY} = \mathbf{g}$ are now easily solved. Set $\mathbf{Y}_{n-1} = \mathbf{g}_{n-1}$ and calculate recursively for $i = n-2, \ldots, 0$

$$\mathbf{Y}_i = \mathbf{g}_i - \mathbf{G}_i\mathbf{Y}_{i+1}\,.$$

Now we have obtained the solution of the set of linear equations (30). With (31) we find $\mathbf{X}(t + \Delta t)$ and therefore the wave function after the timestep Δt. Instead of solving a set of inhomogeneous linear equations where the matrix on the left-hand side has the dimension $N \times N$ with $N = nn_c$ we have to invert only $n_c \times n_c$ matrices. This leads to a much faster procedure even considering that we have to repeat it for each point on the radial grid. In practice, no explicit inversion of matrices is performed because it is numerically more advantageous to solve the corresponding inhomogeneous linear equations, e. g. $\mathbf{B}_{00}\mathbf{G}_0 = \mathbf{B}_{01}$, directly with suitable algorithms.

The integration is started with the (normalized) wave function $\boldsymbol{\Psi}_{M_i}(\vec{r}, t_i) = \boldsymbol{\Phi}_{M_i}(\vec{r}, t_i)$ of the ground state at a time $t_i < 0$ when the time-dependent perturbation $V(\vec{r}, t)$ is negligibly small. The time evolution of the wave function is followed until the perturbation becomes again negligibly small at a time $t_f > 0$ resulting in the wave function $\boldsymbol{\Psi}_{M_i}(\vec{r}, t_f)$ which is still normalized to one but is a superposition of eigenfunctions of $\boldsymbol{H}_0$ with different energies and quantum numbers l_c, J_c, M_c. Note that for each M_i ($M_i = -J_i, \ldots, J_i$) of the initial state the time evolution has to be calculated independently, hence the index M_i.

3. Coulomb Dissociation in the Semiclassical Approximation

3.1. *Time-Dependence of the Perturbation for Coulomb Dissociation*

For the present problem it is sufficient to describe the projectile a in a simple two body model consisting of the fragments b and c with masses m_b, m_c, charge numbers Z_b, Z_c, spins s_b, s_c and position vectors $\vec{r}_b$, $\vec{r}_c$ in coordinate space. The spins can couple to channel spin s with $|s_b - s_c| \leq s \leq |s_b + s_c|$. The interaction between the particles b and c is assumed to depend only on their distance $|\vec{r}|$, so that the Hamiltonian $\boldsymbol{H}_0(\vec{r})$ of the unperturbed system acts only the relative vector

$$\vec{r} = \vec{r}_c - \vec{r}_b. \tag{32}$$

The center-of-mass motion of the projectile is well known [6]. It is treated classically and depends on the initial conditions of the collision, i. e. the projectile velocity v and the impact parameter b. We are only interested in the relative motion of the fragments, which is described by the wave function (3).

The c. m. of the projectile moves on a hyperbolic trajectory in the Coulomb field of the target during the scattering and experiences a time-dependent perturbation

$$V(\vec{r}, t) = \frac{Z_X Z_b e^2}{|\vec{r}_b - \vec{R}(t)|} + \frac{Z_X Z_c e^2}{|\vec{r}_c - \vec{R}(t)|} - \frac{Z_X (Z_b + Z_c) e^2}{|\vec{R}(t)|}, \tag{33}$$

where Z_X is the charge number and $\vec{R}(t)$ the position of the target X relative to the projectile center-of-mass. With $\vec{r}_c = \frac{m_b}{m_b + m_c}\vec{r}$ and $\vec{r}_b = -\frac{m_c}{m_b + m_t}\vec{r}$, a multipole expansion yields

$$V(\vec{r}, t) = \sum_{\lambda\mu} \frac{4\pi Z_X Z_{\text{eff}}^{(\lambda)} e^2}{2\lambda + 1} \frac{r^\lambda}{R(t)^{\lambda+1}} Y_{\lambda\mu}(\hat{r}) Y_{\lambda\mu}^*(\hat{R}(t)) \tag{34}$$

with the effective charge number

$$Z_{\text{eff}}^{(\lambda)} = Z_c \Big(\frac{m_b}{m_b + m_c} \Big)^\lambda + Z_b \Big(-\frac{m_c}{m_b + m_c} \Big)^\lambda. \tag{35}$$

We can integrate out the angular coordinates. Defining

$$C_{c'c}^{\lambda\mu} = \int \mathrm{d}\,\Omega_r \big(\mathcal{Y}_{J_{c'} M_{c'}}^{l_{c'} s}(\hat{r}) \big)^\dagger Y_{\lambda\mu}(\hat{r}) \mathcal{Y}_{J_c M_c}^{l_c s}(\hat{r}) \tag{36}$$

we write

$$\begin{aligned} V(\vec{r}, t) &= \sum_{c'c} \langle \hat{r} | c' \rangle V^{c'c}(r, t) \langle c | \\ \text{with } V^{c'c}(r, t) &= \sum_{\lambda\mu} C_{c'c}^{\lambda\mu} v_{\lambda\mu}(r, t), \end{aligned} \tag{37}$$

where

$$v_{\lambda\mu}(r, t) = \frac{4\pi Z_X Z_{\text{eff}}^{(\lambda)} e^2}{2\lambda + 1} \frac{r^\lambda}{R(t)^{\lambda+1}} Y_{\lambda\mu}^*(\hat{R}(t)). \tag{38}$$

It is convenient to choose the coordinate system in such a way that the z-axis is perpendicular to the scattering plane and the trajectory of the target is symmetric with respect to the x-axis. Then only multipole contributions with even $\lambda + \mu$ appear in the sum.

The position of the target in the projectile c.m. system is given by

$$\vec{R}(t) = \begin{pmatrix} -a(\cosh w + \epsilon) \\ -a\sqrt{\epsilon^2 - 1}\sinh w \\ 0 \end{pmatrix} \quad \text{with} \quad t = \frac{a}{v}(\epsilon \sinh w + w), \tag{39}$$

where the eccentricy ϵ is related to the scattering angle θ (in the center-of-mass system) by

$$\epsilon = \frac{1}{\sin(\frac{\theta}{2})}, \tag{40}$$

and a is half the distance of closest approach in a head-on collision:

$$a = \frac{Z_X(Z_b + Z_c)e^2}{2E_0} \tag{41}$$

with the energy E_0 of the projectile-target c. m. motion. Thus the time dependence of the perturbation is fully specified.

3.2. *Probabilities and Dissociation Cross Sections*

From the known time-dependent wave function $\Psi_{M_i}(\vec{r}, t)$ probabilites of finding the system in individual discrete states can be calculated from the projection of the full wave-function onto the corresponding wave functions. E. g., we have the probability

$$P_k(t) = \left|\langle \Phi_k(\vec{r}, t)|\Psi_{M_i}(\vec{r}, t)\rangle\right|^2 \tag{42}$$

for a given unperturbed state $\Phi_k(\vec{r}, t)$ of the projectile. It is also interesting to study, e. g., the time evolution of the continuum probability

$$P_{\text{cont}}(r, t) = \int \mathrm{d}\,\Omega_r\, r^2\, |\Psi_{\text{cont}}(\vec{r}, t)|^2 \tag{43}$$

with the continuum part of the full wave function

$$\Psi_{\text{cont}}(\vec{r}, t) = \Psi_i(\vec{r}, t) - \sum_k \langle \Phi_k(\vec{r}, t)|\Psi_{M_i}(\vec{r}, t)\rangle \Phi_k(\vec{r}, t) \tag{44}$$

where the sum includes all bound states $\Phi_k(\vec{r}, t)$ of the system.

The triple differential cross section for the Coulomb dissociation of the projectile a into fragments b and c is calculated in the semiclassical approximation as

$$\frac{\mathrm{d}^3\sigma}{\mathrm{d}\,E_{bc}\mathrm{d}\,\Omega_{bc}\mathrm{d}\,\Omega_a} = \frac{\mathrm{d}\,\sigma_R}{\mathrm{d}\,\Omega_a}(\theta) P_{fi}(\vec{q})\varrho_f(q) \tag{45}$$

with the Rutherford cross section

$$\frac{d\sigma_R}{\mathrm{d}\,\Omega_a}(\theta) = \frac{a^2}{4}\left[\sin\left(\frac{\theta}{2}\right)\right]^{-4} \tag{46}$$

for the elastic scattering of the projectile a on the target and the density of final states

$$\varrho_f(q) = \frac{\mu q}{(2\pi)^3\hbar^2} \quad \text{with} \quad q = \frac{\sqrt{2\mu E_{bc}}}{\hbar}. \tag{47}$$

The excitation probability P_{fi} depends on the relative momentum $\hbar q$ between the two fragments and can be calculated in various approximations. In the dynamical calculation discussed here it is given by

$$P_{fi}(\vec{q}) = \frac{1}{2J_i + 1}\sum_{M_i m_s} \left|\langle \Phi^{(-)}_{m_s}(\vec{q}, \vec{r}, t_f)|\Psi_{M_i}(\vec{r}, t_f)\rangle\right|^2, \tag{48}$$

where $\Phi^{(-)}_{m_s}(\vec{q}, \vec{r}, t)$ is a complete scattering solution for the two fragments of the unperturbed Schrödinger equation

$$i\hbar\frac{\partial}{\partial t}\Phi^{(-)}_{m_s}(\vec{q}, \vec{r}, t) = \boldsymbol{H}_0(\vec{r})\Phi^{(-)}_{m_s}(\vec{q}, \vec{r}, t) \tag{49}$$

which asymptotically behaves as a plane wave with momentum $\hbar\vec{q}$ and magnetic spin quantum number m_s and ingoing spherical waves. In general this wave function has the form

$$\Phi^{(-)}_{m_s}(\vec{q}, r, t) = \sum_{\substack{lm_l s \\ JM}} \frac{g^{(-)}_{lsJ}(q, r)}{r}\mathcal{Y}^{ls}_{JM}(\hat{r})(lm_l sm_s|JM) \cdot Y^*_{lm_l}(\hat{q})\exp\left(\frac{E_{bc}t}{i\hbar}\right) \tag{50}$$

which displays explicitly the dependence on the direction of the relative momentum $\hbar\vec{q}$ between the fragments. The wave function $\Psi_{M_i}(\vec{r}, t_f)$ is the solution of the time-dependent Schrödinger equation (12), for $t_f \to \infty$ with the initial condition that for $t_i \to -\infty$

the wave function is just the unperturbed wave function of the ground state $\Phi_{M_i}(\vec{r},t)$. Since one is only interested in breakup contributions it is allowed and advantageous for numerical reasons to replace the full wave function $\Psi_{M_i}(\vec{r},t_f)$ in (48) by the corresponding continuum wave function $\Psi_{\mathrm{cont}}(\vec{r},t)$ (44).

In case of the first order approximation the excitation probability reads

$$P_{fi}(\vec{q}) = \frac{1}{2J_i+1}\sum_{M_i m_s} \cdot \left|\frac{1}{i\hbar}\int_{-\infty}^{\infty} \mathrm{d}\,t\langle\Phi_{m_s}^{(-)}(\vec{q},\vec{r},t)|V(\vec{r},t)|\Phi_{M_i}(\vec{r},t)\rangle\right|^2 . \tag{51}$$

This expression is obtained from (48) if the full time-dependent wave function $\Psi_{M_i}(\vec{r},t_f)$ is replaced by the first-order approximation

$$\Psi_{M_i}(\vec{r},t_f) \approx \Phi_{M_i}(\vec{r},t_f)+\frac{1}{i\hbar}\int_{t_i}^{t_f} \mathrm{d}\,t V(\vec{r},t)\Phi_{M_i}(\vec{r},t). \tag{52}$$

For completeness we also give the excitation probability for the sudden approximation

$$P_{fi}(\vec{q}) = \frac{1}{2J_i+1}\sum_{M_i m_s} \left|\langle\Phi_{m_s}^{(-)}(\vec{q},\vec{r},t)| \cdot \exp\left[\frac{1}{i\hbar}\int_{-\infty}^{\infty} dt\, V(\vec{r},t)\right]|\Phi_{M_i}(\vec{r},t)\rangle\right|^2 . \tag{53}$$

4. Coulomb Breakup of ^{7}Li

The breakup of ^{7}Li during the scattering on heavy targets was first attributed to an electromagnetic process in early experiments of Shotter et al. [14]. After that, Coulomb breakup of ^{7}Li was extensively studied [14 - 16] but a theoretical explanation of the data in the framework of first order theories was not satisfactory. Besides the nuclear contributions to the breakup, higher order effects and the electric quadrupole contribution were suspected to be the main problem. In a recent experiment [12] the Coulomb dissociation of a = ^{7}Li into b = ^{4}He and c = ^{3}H was studied again at a projectile energy of 42 MeV for various targets and scattering angles in order to allow for a systematic investigation of the effects. Therefore, the breakup of ^{7}Li is a good candidate for the application of our method. ^{7}Li is still a rather simple system but it already shows a complex structure with two bound states and conspicious resonances in the continuum. Here, we will investigate higher order effects only in a qualitative way. More detailed calculations with a quantitative comparison to experimental data will appear elsewhere.

Table 1. Depths of the Woods-Saxon potential for various partial waves c.

l_c	0	1	1	2	2	3	3
J_c	1/2	3/2	1/2	5/2	3/2	7/2	5/2
V_c [MeV]	62.74	75.1051	73.4642	64.41	60.42	72.08	64.25

4.1. *Nuclear Model of ^{7}Li*

First, we define the nuclear model of the system in our calculation. ^{7}Li is described in a potential model assuming to consist of ^{4}He and ^{3}H clusters which remain unaffected during the motion. The channel spin s_c is given by the spin $\frac{1}{2}$ of ^{3}H. The wave functions for the αt relative motion are obtained by solving the stationary Schrödinger equation where the Hamiltonian has the form (5) with the reduced mass $\mu = m_\alpha m_t/(m_\alpha + m_t)$. The central potential is assumed to be diagonal in channel space and of Woods-Saxon shape

$$V_0^{c'c}(r) = \frac{-V_c\delta_{c'c}}{1+\exp\left(\frac{r-R}{a}\right)} \tag{54}$$

with radius R = 2.39 fm and diffuseness parameter a = 0.68 fm. The depth of the potential V_c is adjusted in the partial waves with l_c = 1 and l_c = 3 to give the correct energy of the bound states and the resonances, respectively. For l_c = 0 the depth was adjusted to give approximately the experimental scattering phase shifts. In the case of the partial waves with l_c = 2 we use the depth of partial wave l_c = 0 and additionally a mean spin-orbit potential deduced from the depths of the potentials in partial waves l_c = 1 and l_c = 3 for different J_c. The values for V_c are given in Table 1. Now all free parameters of our model are fixed. The model space in our calculation is restricted to s-, p-, d-, and f-waves. Besides the physical bound states in partial waves with l_c = 1 there are also unphysical bound states in our model, e. g. a $(1/2)^+$ state at -8.27 MeV, a $(5/2)^+$ state at -7.37MeV and a $(3/2)^+$ state at -5.42 MeV. In the calculation of the time-

	Theory	Experiment [17, 18]
Energy E / MeV of ground state ($\frac{3}{2}^-$)	–2.4678†	–2.4678
Energy E / MeV of first excited state ($\frac{1}{2}^-$)	–1.9902†	–1.9902
Energy E / MeV of $\frac{7}{2}^-$ resonance	2.1622†	2.1622
Energy E / MeV of $\frac{5}{2}^-$ resonance	4.2122†	4.2122
Width Γ / keV of $\frac{7}{2}^-$ resonance	88.3	(93 ± 8)
Width Γ / keV of $\frac{5}{2}^-$ resonance	862	(875^{+200}_{-100})
Electric quadrupole moment of ground state Q_e	–43.1 mb	(-40.6 ± 0.8) mb
B(E2, $\frac{3}{2}^- \rightarrow \frac{1}{2}^-$) / e^2fm^4	6.15	(8.3 ± 0.5)
Astrophysical S-factor S(0) / keVb	0.1068	(0.1067 ± 0.0068)
Branching ratio R (DC $\rightarrow \frac{1}{2}^-$ / DC $\rightarrow \frac{3}{2}^-$)	0.429	(0.453 ± 0.020) (0.437 ± 0.022)

Table 2. Properties of the ^{7}Li system in the assumed potential model. (†: fitted to experimental value).

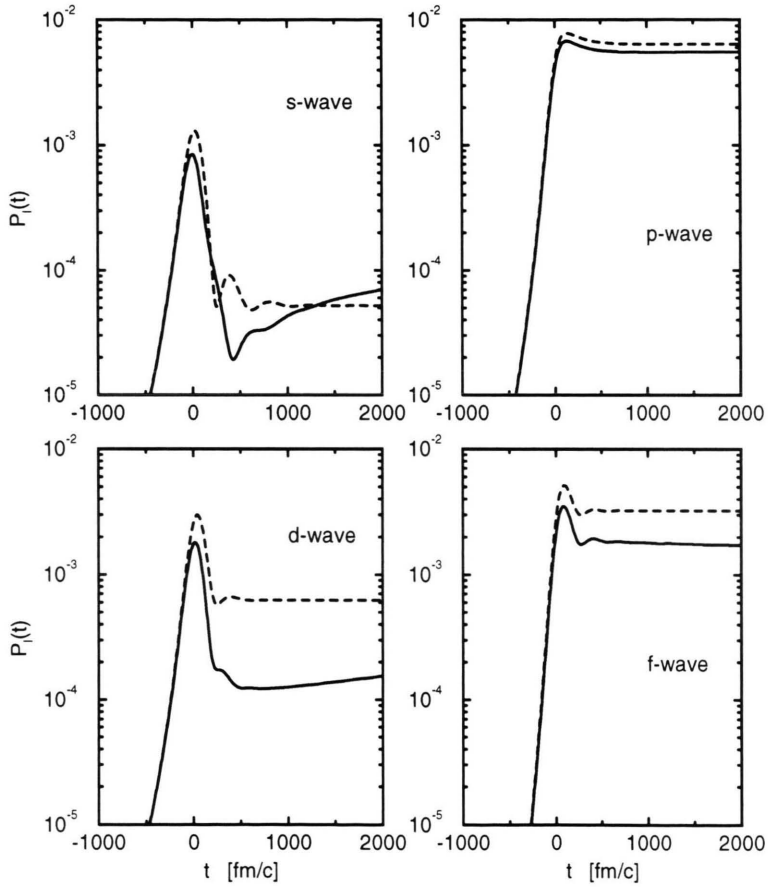

Fig. 1. Time-evolution of the probability $P_l(t)$ in various partial waves l with the initial channel ($J = \frac{3}{2}$, $M = \frac{3}{2}$). In case of the p-wave the initial channel is not included. First order results are given by dashed lines and results of the dynamical calculation by solid lines. Time $t = 0$ is at the distance of closest approach.

evolution with perturbation we have to guarantee that these states are not populated. This is done after each time step by projecting out the forbidden states from the wave functions of the respective channels and by the amplitude of the initial state accordingly.

From the wave functions several properties of the system can be calculated. They are given in Table 2. The widths of the continuum resonances are close to the experimental values. The electric quadrupole moment of the ground state and the B(E2) values for the transition from the ground to the first excited state are mainly determined by the inner part of the wave function while the astrophysical S-factor is sensitive to the outer parts of the ground state wave function.

Even in our simple model the ^{7}Li system is rather well described.

4.2. *First Order vs. Dynamical Calculation of Coulomb Dissociation*

As an example for the application of the method, we will now study the Coulomb breakup of 42 MeV ^{7}Li scattered on ^{197}Au for a scattering angle of 50°. In the semiclassical approximation this corresponds to an impact parameter of 8.7 fm and a minimal distance between target and projectile of 13.9 fm at closest approach. The Sommerfeld parameter, (1), with $\eta = 15.3$ is large enough to justify this approximation. The adiabaticity parameter, (2), $\xi \approx 1$ at breakup threshold limits the probability for excitation to continuum states.

In the dynamical calculation we use a mesh with 1200 equidistant points of distance 0.3 fm for each of the channel wave functions. Due to the selection rules from the choice of our coordinate system we have a maximum of 16 coupled channels in a calculation with given M_i when we consider s-, p-, d- and f-waves. We have 4 possible initial states ($M_i = -3/2, \ldots, 3/2$) for the ground state total angular momentum of $J_i = 3/2$. The time-integration is started with the projectile-target distance of 120 fm with a step-size of $\approx$ 8 fm/c. After passing the moment of closest approach, the evolution of the wave function is followed up to a time when the distance reaches at least 300 fm. In the multipole expansion of the Coulomb interaction (34) we only consider E1 and E2 contributions.

Let us first examine the time-evolution of various probabilities when we start with the initial state $J_i = 3/2, M_i = 3/2$. In Fig. 1 we show the total probability

$$P_l(t) = \int \mathrm{d}^3 r \left| \sum_c \delta_{ll_c} \frac{\psi_c(r,t)}{r} \mathcal{Y}^{l_c s_c}_{J_c M_c}(\hat{r}) \right|^2 \qquad (55)$$

of finding the system in a single partial wave l as a function of time. In case of the p-wave we consider all states except the initial state. The time-dependence displays a distinct structure. Before the time of closest approach of projectile and target ($t = 0$ fm/c) the probabilities in the first order calculation and in the dynamical calculation are very similar. They rise very steeply and show a pronounced maximum around $t = 0$ fm/c, especially in the s- and d-waves. For later times the difference between the two calculations becomes larger, displaying the importance of higher order effects. The oscillatory structure in the first order calculation, e. g. for the s-wave probability, is related to the exponential time dependence $\exp(i\omega_{fi}t)$ in the first order amplitude (cf. (51)). Here the excitation energy $\hbar\omega_{fi}$ enters which is typically about 3 MeV which corrresponds to a period of $\approx$ 400 fm/c. The first order probabilities converge rather fast to their final values whereas the probabilities in the dynamical calculation change appreciably even for large times. This can be understood from the spatial extension of the system which interacts with the external perturbation. In case of the first order calculation the probability is given by the overlap between the initial bound state wave function and the time-dependent perturbing potential at all times whereas in the dynamical calculation the full wave function enters which includes bound and scattering wave functions. The linear combination of these results in a wave packet which spreads out in the course of time (see below). From Fig. 1 we also see that the excitation probability is larger in the first order calculation than in the dynamical calculation (except for the s-wave). For p- and d-waves which can be populated in the first order calculation only by E2 transitions we find a "dynamical quenching" similar to the observation in [11] in the Coulomb breakup of ^{8}B. Also, the d-wave probability is reduced in the dynamical calculation.

Figure 2 displays the time-evolution of the angular integrated probability in the continuum (43) for the two methods of calculation and the initial state $J_i = 3/2$, $M_i = 3/2$. The quantity $\log[P(r,t)]$ is given for $P(r,t) \geq 10^{-7}$ fm^{-1} as a function of r and t where the starting time of the integration is approx. –1141 fm/c. At first sight the time-dependence of the radial probability looks rather similar in both calculations. At times before the closest approach of target and projectile, i. e. $t = 0$ fm/c, the excitation leads to an increase of the probability for small values of r corresponding to the spatial extension of the initial state. The probability reaches a maximum shortly after $t = 0$ fm/c. After that a wave packet starts to propagate outwards but at the same time a large fraction of the probability remains in the nuclear interior. This corresponds dominantly to the excitation of the $(7/2)^-$ resonance in the continuum which has a mean lifetime of approx. 2.1×10^3 fm/c or 7.1×10^{-21} s. Once a state in the continuum is excited, in the first order calculation the respective wave function evolves under the action of the free Hamiltonian (5) without

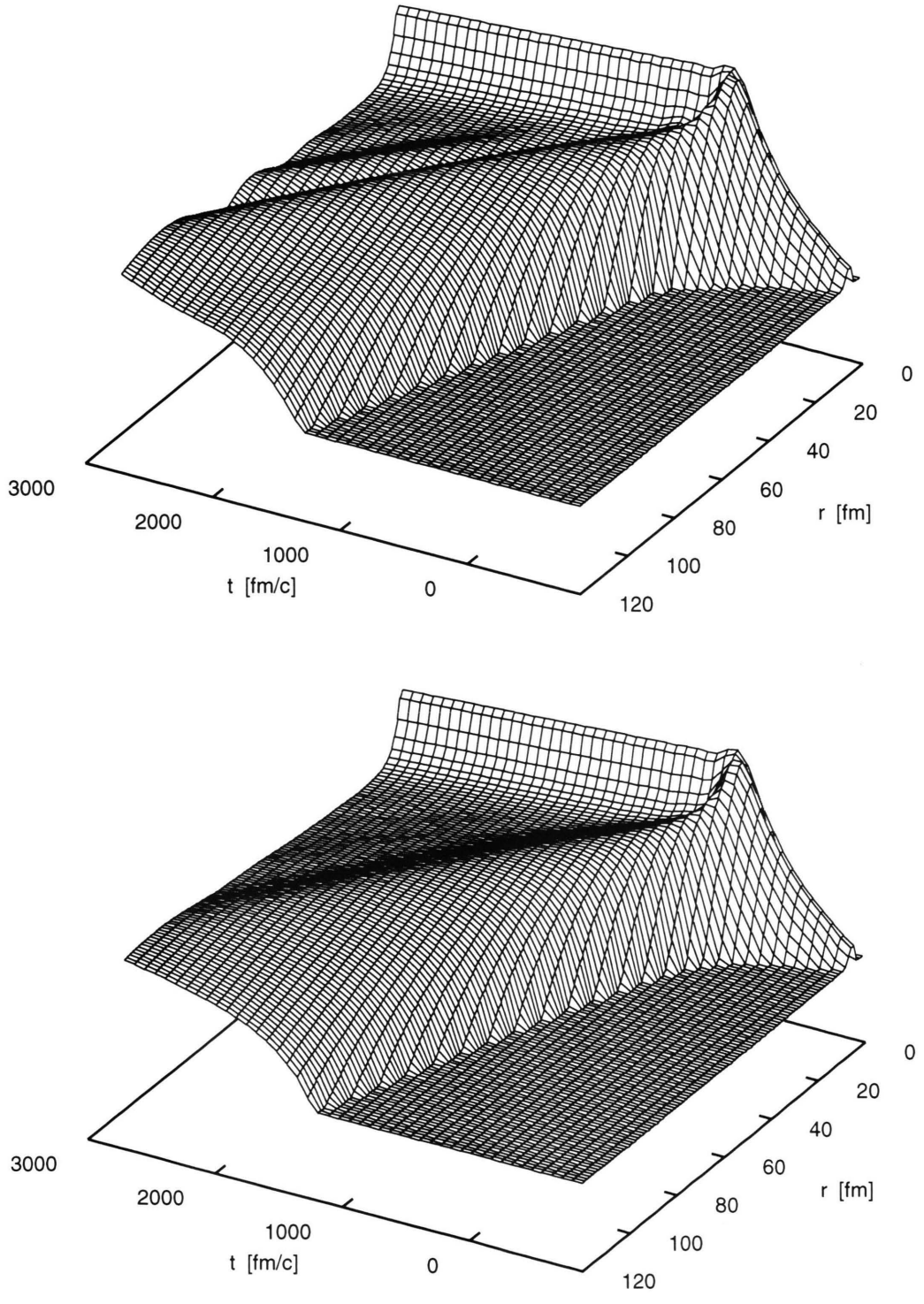

Fig. 2. Time-evolution of the probability of the system to be in the continuum $P_{\mathrm{cont}}(r,t)$ in the first order calculation (top) and the dynamical calculation (bottom). See text for a detailed explanation.

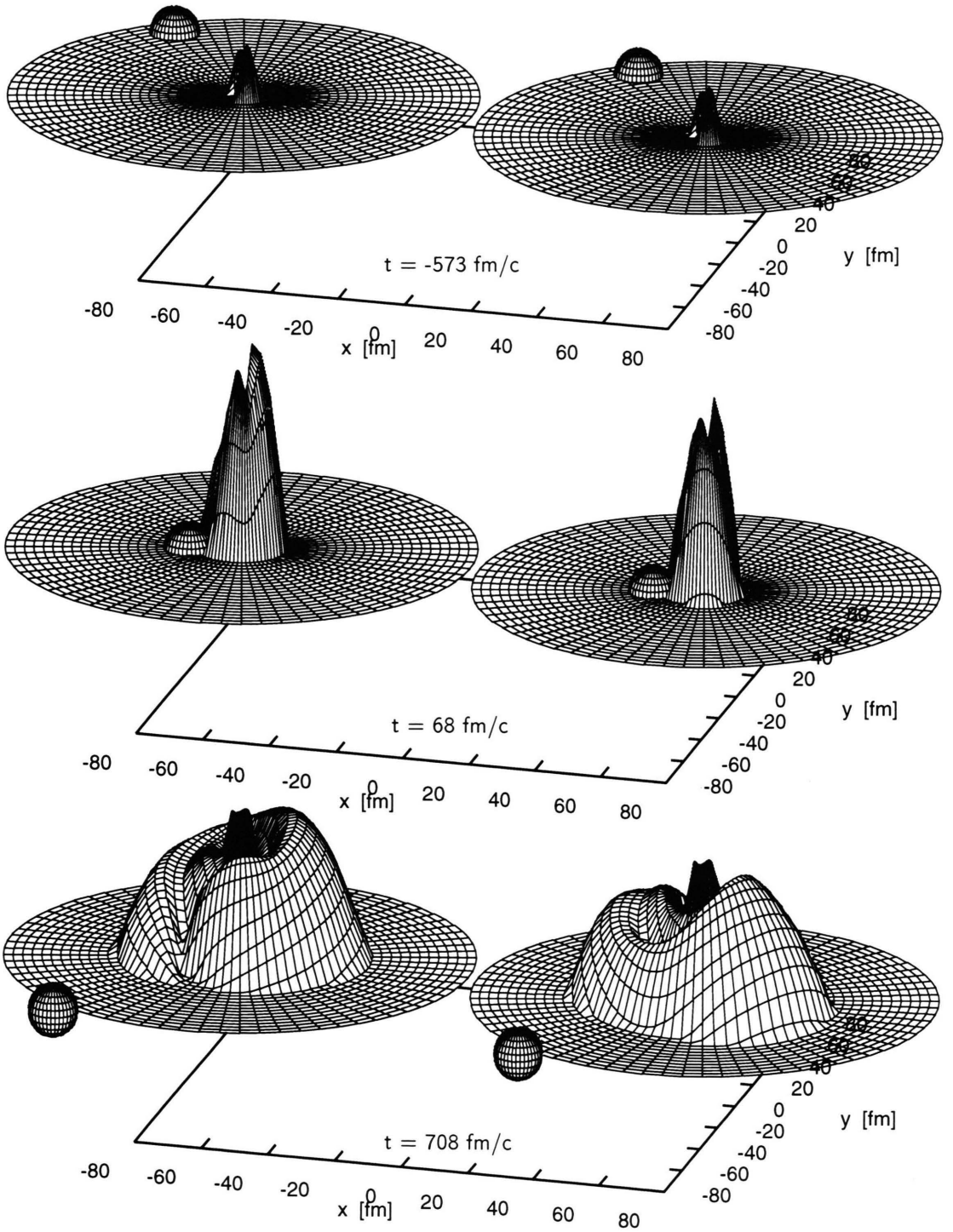

Fig. 3. Time-evolution of the probability $P_{\mathrm{cont}}(r_t, \phi, t)$ in the first order calculation (left) and in the full dynamical calculation (right). The position and size of the target in the scattering plane is indicated by a sphere at each moment. See text for a detailed explanation.

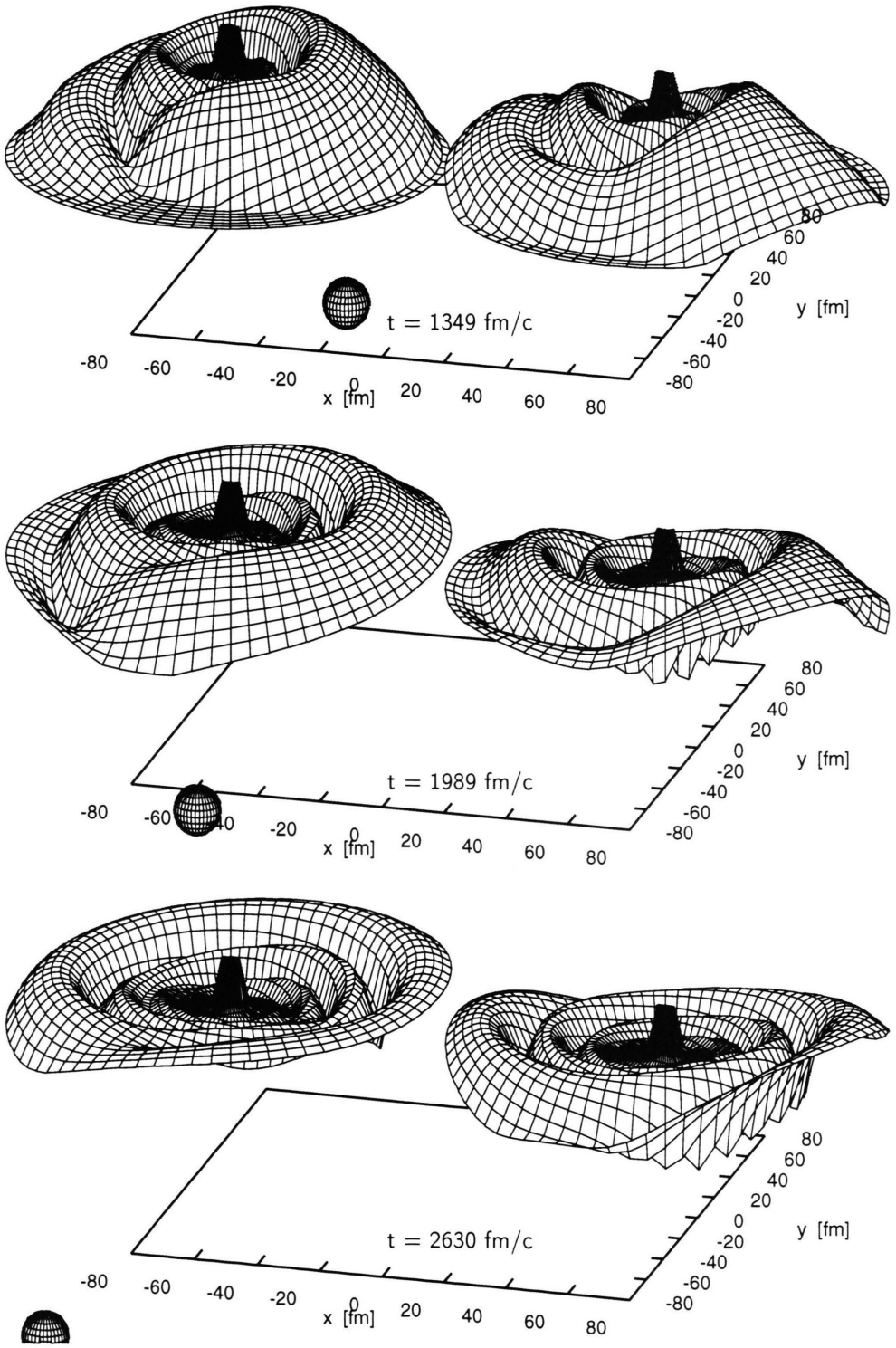

Fig. 4. The same as in Fig. 3 but for later times.

interacting with other states anymore. In contrast, in the dynamical calculation the continuum states are perturbed by the time-dependent potential. This explains the difference in the shapes of the wave packet in the two calculations at large times.

The influence of higher order effect becomes more distinct when we study the time-evolution of the probability of finding the triton at a distance r_t from the c.m. of the projectile at an angle ϕ. It is given by

$$P_{\mathrm{cont}}(r_t, \phi, t) = \frac{1}{\varrho} P_{\mathrm{cont}}\left(\frac{r_t}{\varrho}, \phi, t\right)$$
$$\text{with } P_{\mathrm{cont}}(r, \phi, t) = \int \mathrm{d}\cos(\theta)\, r^2 \left|\Psi_{\mathrm{cont}}(\vec{r}, t)\right|^2 \tag{56}$$

and $\varrho = m_\alpha/(m_\alpha + m_t)$. Note that the z-axis is perpendicular to the scattering plane in our coordinate system. In Figs. 3 and 4 the quantity $\log[P(r_t, \phi, t)]$ for $P(r_t, \phi, t) \geq 10^{-7}$ fm^{-1} in the first order calculation is compared to the result of the dynamical calculation for different times in the time-evolution. For $t < 0$ fm/c the probability increases at small r_t and there is hardly a difference in the two distributions. At $t = 68$ fm/c the distributions are still rather compact but differences can be noticed. The tail of the probability distribution overlaps with the target because of the small impact parameter. At $t = 708$ fm/c we find a central peak in the probability from the continuum resonances. Additionally, the wave packet starts to spread out. Here, we already see that the angular distribution for the emission of the trition in the projectile system differs very much in the two calculations. In the first order calculation the triton is emitted preferably in a direction approximately opposite to the target while this direction is rotated in the full calculation. The angular distribution is determined by the inference of the various partial waves. For later times the wave packet continues to spread out and develops a spiral-like structure.

Finally, in Fig. 5 we compare the double differential breakup cross section

$$\frac{\mathrm{d}^2\sigma}{\mathrm{d}E_{\alpha t}\mathrm{d}\Omega_{\mathrm{Li}}} = \int \mathrm{d}\Omega_{\alpha t} \frac{\mathrm{d}^3\sigma}{\mathrm{d}E_{\alpha t}\mathrm{d}\Omega_{\alpha t}\mathrm{d}\Omega_{\mathrm{Li}}} \tag{57}$$

for various partial waves in the two calculations. For low relative energies the s-wave contribution dominates the cross section. With increasing energy contributions from additional partial waves become more important. The $(3/2)^-$ resonance in the f-wave stands

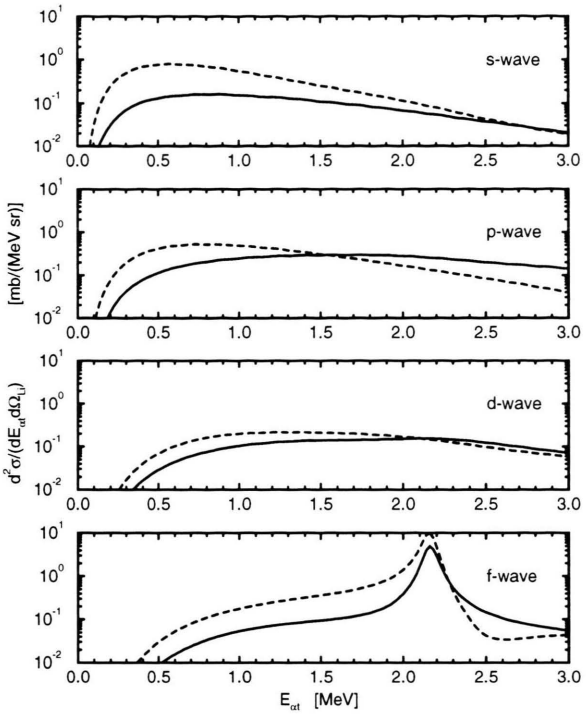

Fig. 5. Double differential cross section for the Coulomb breakup of 42 MeV ^{7}Li into α and t scattered on ^{179}Au at 50° as a function of the αt relative energy for various partial waves. Results of the full dynamical calculation (solid lines) and of the first order calculation (dashed lines).

clearly against the continuum. Higher order effects have a strong impact on the cross sections. For small relative energies they reduce the cross section but for higher energies the results in the dynamical calculation become larger than in the first order calculation. So both the absolute value and energy dependence of the cross sections change appreciably.

5. Summary and Conclusions

For the first time higher order effects in the Coulomb dissociation of ^{7}Li were investigated in a fully dynamical description of the excitation process. For this purpose we have studied the time evolution of the projectile system in the semiclassical approximation of Coulomb breakup. The corresponding time-dependent Schrödinger equation was solved with an efficient numerical algorithm which can also be applied to other time-dependent problems. In principle, it is possible with our method to study systematically the dependence of higher order effects on

experimental conditions. This can help to determine a suitable range of projectile energies, scattering angles and target charges. Here, we limit ourselves to first exploratory calculations.

As an example where higher order effects are expected to be of great significance, we chose the conditions of a recent experiment with a ^{7}Li projectile with a rather small energy of 42 MeV, a scattering angle of 50°, and a ^{197}Au target. For the description of the ^{7}Li system we used a simple but rather accurate potential model which allows to treat in a consistent way both bound and scattering states, including resonances. As there is no experimental information on the E2 strength in the continuum we have to rely on the predictions of our model.

We compared the time-dependence of various probability distributions in the full dynamical calculation with first order results in order to get an impression of the effects of higher order contributions to the breakup. Indeed, they have a strong influence on the results in the chosen example by changing the absolute value of cross sections and even more importantly the angular distribution of the fragments. This has to be considered in a reliable application of the Coulomb dissociation method.

Our method is sufficiently flexible to allow for various extensions in the calculation. The number of multipole contributions can be extended beyond E1 and E2, and higher partial waves than $l = 0, \ldots, 3$ can be included with the consequence of an increased complexity of the calculation. Nuclear contributions to the breakup were not, but can be included since they can be significant for large scattering angles. The dissociation of other nuclei of interest, like ^{8}B, can also be studied in the framework of our model. Higher order effects are fully taken into consideration in the time-dependent treatment of Coulomb breakup. Therefore it is possible to obtain information on radiative capture reactions with sufficient accuracy, which is necessary for a reliable foundation of astrophysical models.

[1] G. Baur, C. A. Bertulani, and H. Rebel, Nucl. Phys. **A458**, 188 (1986); G. Baur and H. Rebel, J. Phys. G: Nucl. Part. Phys. **20**, 1 (1994); Annu. Rev. Nucl. Part. Sci. **46**, 321 (1996).

[2] S. Typel and G. Baur, Nucl. Phys. **A573**, 486 (1994); Phys. Rev. **C50**, 2104 (1994); S. Typel, H. H. Wolter, and G. Baur, Nucl. Phys. **A613**, 147 (1997).

[3] C. A. Bertulani and L. F. Canto, Nucl. Phys. **A539**, 163 (1992); L. F. Canto, R. Donangelo, A. Romanelli, and H. Schulz, Phys. Lett. **B318**, 415 (1993).

[4] G. Süßmann, Einführung in die Quantenmechanik, B.I.-Hochschultaschenbuch Bd. 9/9a, Bibliographisches Institut, Mannheim 1963.

[5] J. Schneider, Subbarrierenfusion als Tunneln von mehrdimensionalen Wellenpaketen, Dissertation, Ludwig-Maximilians-Universität, München, 1987; J. Schneider and H. H. Wolter, Z. Phys. **A 339**, 177 (1991).

[6] K. Alder, A. Bohr, T. Huus, B. Mottelson, and A. Winther, Rev. Mod. Phys. **28**, 432 (1956).

[7] G. F. Bertsch and C. A. Bertulani, Nucl. Phys. **A556**, 136 (1993); Phys. Rev. **C 49**, 2839 (1994).

[8] T. Kido, K. Yabana, and Y. Suzuki, Phys. Rev. **C 50**, R1276 (1994).

[9] H. Esbensen, G. F. Bertsch, and C. A. Bertulani, Nucl. Phys. **A581**, 107 (1995).

[10] C. A. Bertulani, Nucl. Phys. **A587**, 318 (1995).

[11] H. Esbensen and G. F. Bertsch, Nucl. Phys. **A600**, 37 (1996).

[12] H. Utsunomiya et al., Phys. Lett. **B416**, 43 (1998); K. Osada, Master thesis, Konan University, Kobe, 1998.

[13] S. E. Koonin and D. C. Meredith, Physik auf dem Computer 2, R. Oldenbourg Verlag, München 1990.

[14] A. C. Shotter et al., Phys. Rev. Lett. **46**, 12 (1981); Phys. Lett. **53**, 1539 (1984); J. Phys. G: Nucl. Phys. **14**, L169 (1988).

[15] H. Utsunomiya et al., Phys. Lett. **B211**, 24 (1988); Nucl. Phys. **A511**, 379 (1990); Phys. Rev. Lett. **65**, 847 (1990), **69**, 863(E) (1992).

[16] J. Yorkston et al., Nucl. Phys. **A524**, 495 (1991); S. B. Gazes et al., Phys. Rev. Lett. **68**, 150 (1992); J. E. Mason et al., Phys. Rev. **C45**, 2870 (1992).

[17] F. Ajzenberg-Selove, Nucl. Phys. **A490**, 1 (1988).

[18] C. R. Brune, R. W. Kavanagh, and C. Rolfs, Phys. Rev. **C50**, 2205 (1994).